JOURNAL OF MATERIALS SCIENCE **40** (2005) 5845–5851

The wet Kelvin model for air flow through open-cell polyurethane foams

N. J. MILLS
Metallurgy and Materials, University of Birmingham, UK
E-mail: n.j.mills@bham.ac.uk

Computational Fluid Dynamics (CFD) was used to compute the air-flow permeability K for laminar flow, for wet Kelvin foam models, as a function of cell size and cell face hole size. The predictions were compared with experimental data for a range of open-cell polyurethane (PU) foams. This suggests that the foam permeability is a function of the area of largest hole in the cells. The predictions are almost the same as those for dry Kelvin foams, showing that the face hole size and cell size are the main factors that determines foam permeability.

1. Introduction

The microstructures of polyurethane (PU) foams range from reticulated low density foams, where no cell faces remain, to foams with small circular holes in the centre of the cell faces. The latter often are slow-recovery foams, used for seating and mattress toppers. The aim of this paper is to improve the modelling of air-flow through such foams.

Air flow measurements are used to characterise the open-cell content of PU foams. Air flow also affects the compressive impact response [1] of foam blocks of diameter exceeding 0.5 m, at velocities exceeding 5 m s^{-1}. Jones and Fesman [2], and Gent and Rusch [3], described air-flow measurements on open-cell PU foams. They correlated these with microstructural parameters such as cell size, the proportion of open cell faces, and foam density. The equation used for the pressure gradient causing unidirectional steady-state flow was

$$\frac{\Delta P}{L} = \frac{\eta}{K} V + \frac{\rho}{B} V^2 \tag{1}$$

where ΔP is the pressure drop across a foam length L, V the air velocity, η the air viscosity $= 18 \times 10^{-6}$ Pa s, and ρ its density $= 1.29$ kg m^{-3}. They showed that the permeability K (m^2) and the inertial flow coefficient B (m), for several types of open-cell PU foam, were functions of the applied compressive strain. Hilyard and Collier [4] attributed the first term on the right hand side of Equation 1 to laminar air-flow, and the second to turbulent air-flow. Mills and Lyn [1] measured the air-flow through PU chip foams (remoulded from a mixture of hardnesses of upholstery foams) for a range of flow velocities, and evaluated the parameters B and K as a function of foam compression.

Lord Kelvin [5] proposed a tetrakaidecahedral cell model for the structure of soap foams, which he claimed had a minimum surface energy. Each cell consists of six square and eight regular-hexagonal faces, and every edge has the same length. The edges meet at tetrahedral vertices. The cell centres are on a body centred cubic (BCC) lattice. Brakke and Sullivan [6] and Kraynik *et al.* [7] used Surface Evolver software to create the geometry of foam cell structures. Such foams are described as 'wet' if there is a finite volume fraction of liquid, and as 'dry' if the liquid volume fraction in the vertices and edges is negligible.

Gent and Rusch [3] proposed a qualitative model for the air-flow resistance of flexible PU foams. In this, air or liquid flows down a pipe, with diameter equal to the cell diameter D, containing round orifices at spacing D. However, prior to the advent of computational fluid dynamics (CFD), they were unable to consider the velocity distribution across the pipe, or the effect of one constriction on the pressure drop at the next constriction. They predicted a permeability that was unaffected by the hole area

$$K = \frac{D^2}{32} \tag{2}$$

Turbulent air-flow should not occur unless the Reynolds number $Re > 2000$. For experimental measurements on foams, in which the flow velocity is 5 m s^{-1} and the cell diameter is 1 mm, $Re = 350$. Hence the air flow in the foams should be laminar.

Fourie and Du Plessis [8] considered both streamline and turbulent air-flow through open-cell aluminium foams. They calculated the air resistance of a single strut in an infinite chamber; and counted the number of such obstacles in the Kelvin foam model. Consequently they did not use periodic boundary conditions. Their predicted permeability is a function of the foam tortuosity, a quantity with an ambiguous definition.

0022-2461
DOI: 10.1007/s10853-005-5018-5

TABLE I Foams tested

Manufacturer	Trade name	Density kg m^{-3}	Relative density R	Stress at 20% compression kPa
Royal medica	Part of cushion	130.8	0.108	6.8
Dynamic systems	Sunmate soft	87.0	0.072	5.6
	Sunmate medium	79.9	0.066	13.7
	Sunmate firm	82.3	0.069	20.9
Dynamic systems	Pudgee	221.9	0.185	2.7

TABLE II Parameters from image analysis of foam sections

Foam	Cell diameter D_C^s μm	Hole diameter D_H μm	D_H/D_C	hole area 10^4 μm^2
Royal Medica	300 ± 110	78 ± 52	0.42	0.70 ± 1.04
Sunmate soft	290 ± 180	51 ± 4	0.29	0.34 ± 0.69
Sunmate medium	280 ± 100	34 ± 27	0.19	0.15 ± 0.24
Sunmate firm	290 ± 90	29 ± 15	0.16	0.085 ± 0.08
Pudgee	330 ± 180	87 ± 75	0.42	0.91 ± 2.60

Boomsma *et al*. [9] used CFD to calculate the permeability of a 'wet' Weaire-Phelan foam, with a single mean cell size and relative density, as a model for water flow through a open-cell aluminium foam. Fitzgerald *et al*. [10] modelled air flow through PU foams having circular holes in the faces, using a 'dry' Kelvin foam model. The flow was directed along the [001] axis of the BCC lattice, and symmetry was used to reduce the size of the structure analysed. Their predictions were within a factor of 3 of the experimental data. However they ignored the curvature of the Plateau border [11] edge cross-sections, which may influence the air permeability. Since the permeability was computed for a single flow direction, it was not possible to assess whether the permeability was isotropic.

2. Foams and their microstructure

The slow recovery PU foams characterised by Fitzgerald et al.[10] are listed in Table I. The relative density values are based on a nominal PU solid density of 1200 kg m^{-3}. The Sunmate foams, from Dynamic Systems Inc (Leicester, NC, USA), have elongated cells as a result of foam rise during manufacture; the cells are approximately polyhedral. The denser Pudgee foam, and The Royal Medica (Italian) foam from a wheelchair cushion, have a different microstructure in which the bubbles maintain their spherical shape, rather than being polyhedral. Typical SEM images of the two foam types are shown in Fig. 1. The relative densities of the Sunmate foams are $R \approx 0.07$, whereas they are significantly higher for the other foams.

The factors that control air-flow are the size of holes in cell faces, their orientation and spacing, the cell size, and the fraction of faces that contain holes. Table II shows that the mean diameter of sectioned cells is close to 300 μm for all the foams. However, the sectioning process cuts cells at random positions. If the cells were uniform in size, the mean cell diameter would be 1.62 times the mean diameter of sectioned cells. Therefore the mean cell diameter is approximately 0.5 mm for all the foams. The mean hole area is smaller for the Sunmate foams than for the others. The ratio of the hole diameter to the cell diameter D_H/D_C, given in the last column of Table II, has been calculated assuming that $= 1.62\ D_C^s$

3. Generating the wet Kelvin foam geometry using Surface Evolver

The file *twointor.fe* (Surface Evolver website at //www.susqu.edu/facstaff/b/brakke/evolver/) lists 12 vertices, 24 edges, 14 triangular faces, and 2 bodies that are repeated in toroidal space, to create the dry Kelvin closed-cell foam. The foam cells have diameter D, between two square faces, of 1 unit. All the cell edges have length L, while cell diameter, between two parallel square faces, is $2\sqrt{2}L$ (Fig. 2a).

A *wetfoam.cmd* command is used to create an 'initial' wet structure; an edge spread parameter determines the width of the equilateral triangular section edges, which replace the line edges of the dry foam. The wet structure is 'evolved,' increasing the number of triangular faces that approximate the shape of the curved air-liquid interface, then iterating to minimise the surface energy. The sequence of commands 'gogo' in the *wetfoam* file was used once, giving a good approximation to the foam shape without creating an excessive number of faces. It consists of {g 5; r; g 5; hessian; r; g 5; hessian; hessian;} where:g: iteration step in which the vertices are moved; g5 means 5 iterations. r; refine the triangulation; edges are divided in two, and faces into four. Hessian; one iteration in which the second derivative matrix for energy is calculated, then solved for the minimum energy.

In the evolved structure, the infinitesimally-thin, flat, two-sided faces (that are not listed as *density* = 0.5) were removed from the.fe data files, creating near-circular holes in the cell faces (Fig. 2b). The edge spread parameter affects the face hole size and the foam relative density R (Table III). The square face hole diameter is also given in terms of L. However, if the edge spread $S > 0.4$, the evolution process causes the square faces to remain wet (a fact noted by Phelan, Weaire and Brakke [12]), so no holes exist in these faces. This upper limit is above that of the commercial PU foams used in cushions.

The toroidal space used by Surface Evolver is not understood by GAMBIT or CAD programs. Consequently the evolved wet Kelvin structure was converted into a form that can be read by such programs. First

TABLE III Parameters of evolved wet Kelvin foams

		in D (cell diameter) units		in L units
Edge spread S	Relative density R	hexagonal face hole diameter	Square face hole diameter	Square face hole diameter
0.1	0.00691	0.540	0.336	0.951
0.2	0.0276	0.478	0.263	0.743
0.3	0.0622	0.409	0.181	0.512
0.35	0.0846	0.376	0.140	0.395
0.4	0.1105	0.340	0.095	0.268

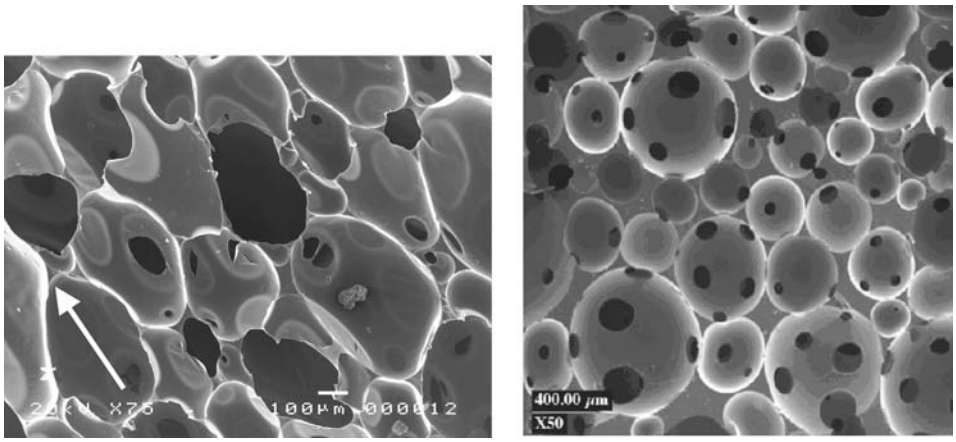

Figure 1 SEM foam microstructures: left Sunmate medium, right Pudgee. The sheet normal direction in the Sunmate foam is shown by the arrow.

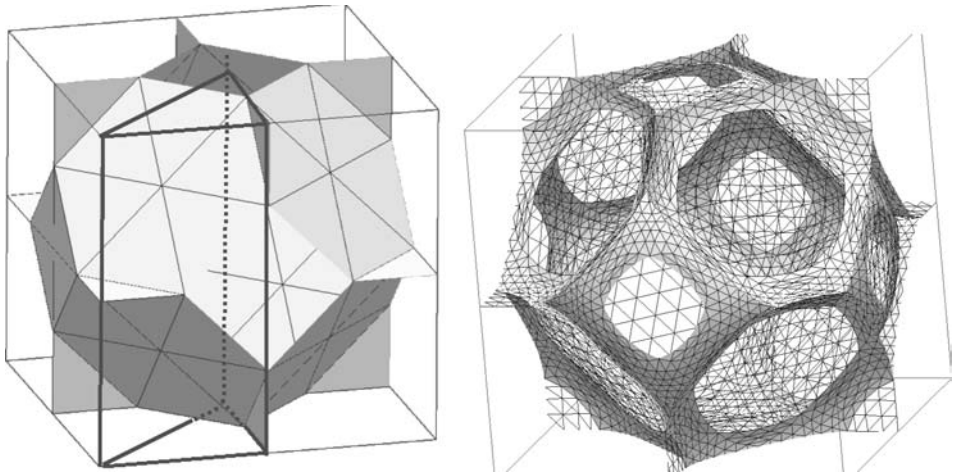

Figure 2 Complete cells of a) dry Kelvin closed-cell foam, (b) wet Kelvin open-cell foam, for edge width parameter $S = 0.2$. The surrounding cube is the BCC unit cell. In a) the prism for the [001] direction air flow CFD is shown; in b) the edges of facets that form part of the face holes are still visible.

the torus edge wrap conditions were interpreted to give the Cartesian coordinates of vertices connected by 1 edge to a vertex inside the prism, then Javaview (available from www.javaview.de) used to convert the.fe file to a wavefront.obj file. Next, Rhinoceros CAD (Robert McNeel & Associates, Seattle) was used to convert it to an ACIS.sat file that could be read by GAMBIT. The boundaries of the prism for CFD were used to cut out the required part of the evolved structure. The polymer volume was then subtracted from the prism to leave a volume representing the air space in the foam. In the model all the cell faces have holes, and all the cells are of equal size.

4. CFD of air-flow through the foams

Computational fluid dynamics (CFD) is used to evaluate the velocity fields under a given pressure gradient. The 3-Dimensional version of the program Fluent 6 (Fluent Inc, Lebanon, New Hampshire, USA) was used, with the pre-processor Gambit to create the geometry and the mesh. Fluent 6 allows periodic boundary conditions, at pairs of face boundaries that are parallel, and which have identical meshes. In the real foam there is a constant pressure gradient in the permeability, apart perhaps at the surface layers. In the regular cell models, this pressure gradient is applied to the repeating unit. Laminar air-flow conditions were chosen.

Mechanics analysis [13] showed that the Kelvin open cell foam is nearly elastically isotropic, with the greatest Young's modulus being in the [001] direction and the smallest in the [111] direction of the BCC lattice. It was assumed that these directions would also be maxima or minima for air permeability, so computations were made in these directions. The high degree of symmetry in these directions allows the analysis of a relatively small repeating unit.

4.1. CFM of flow in the 001 direction

For air-flow in the [001] direction of the Kelvin foam, there is a 4–fold rotational symmetry axis along [001] at the centre of the square faces (Fig. 2a), and there are two mirror planes containing [001]. Hence it is only necessary to consider the triangular prismatic unit, of length $2\sqrt{2}\,L$, shown in Fig. 3a. Alternatively a prism of length $\sqrt{2}L$ can be used (Fig. 4a), since the flow pattern in the two halves of the longer prism are related by mirror symmetry. The two orthogonal prism sides have width $\sqrt{2}L$, while the diagonal side has width $2L$. The prism contains parts of three cells: 1/8th of a cell with a square face at the entry and exit of

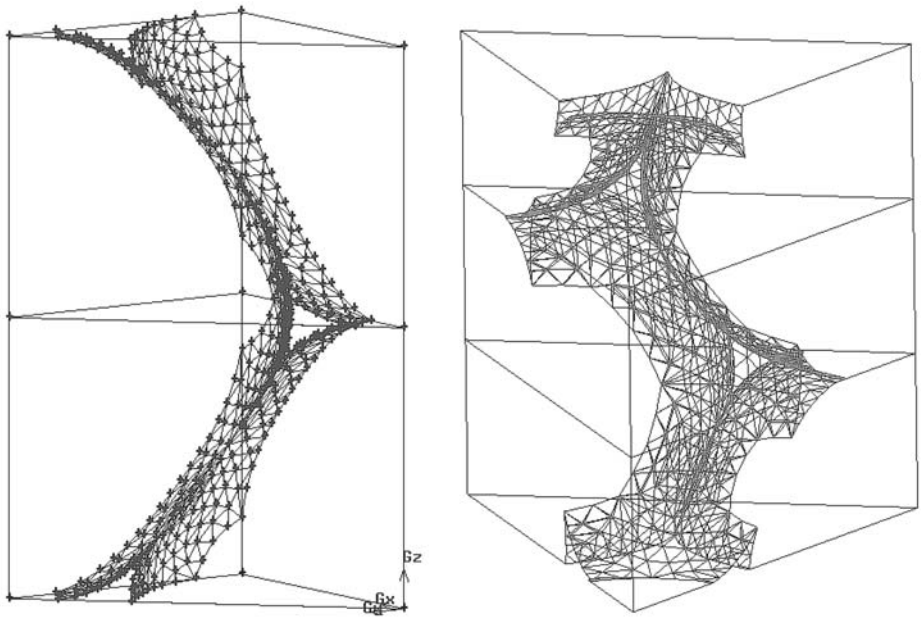

Figure 3 Prisms used for CFD: (a) [001] direction, edge spread $S = 0.2$, (b) [111] direction, $S = 0.3$. The air flow is in the vertical z direction. The lateral prism faces are mirror symmetry planes, while those at the top and base are periodic boundaries.

the unit, and two 1/16th cells, separated from the first by holes in half hexagonal faces, and from each other by a hole in an 1/8th square face. There are mirror symmetry boundary conditions for the flow vectors, on the prism sides, which meet at 45° and 90°. The diagonal prism side is at the front of Fig. 3a, while the smaller sides contain parts of holed square faces. The mesh of triangles defines the surface of the polymer; a cut Plateau border section can be seen at the prism boundary, and cut half sections at the top and base. There are periodic boundary conditions on the prism end faces.

In prior CFD research [10], the mesh size was reduced until the predicted flow integrals became independent of the mesh size; this showed that the side of the tetrahedral elements should be less than 0.05 of the cell edge length L. The SIMPLE algorithm was used in FLUENT, with a first order upwind discretization scheme, and the default over-relaxation factors. The iteration was continued until the residual velocity was $< 10^{-5}$ m s^{-1}; the flow rates were also monitored, and checked for convergence. CFD with a second-order upwind discretization scheme produced the same flow rate.

The flow rate Q was computed, as the sum of the surface integrals of the z velocity component on the two periodic boundaries (a hole and a cell midplane). The mean air velocity $\overline{V}$ in the foam is Q divided by the cross sectional area of the prismatic unit. It is substituted in the first part of Equation 1 to compute the foam permeability

$$K = \eta \overline{V} \Big/ \frac{\Delta P}{L} \tag{3}$$

4.2. CFM of flow in the [111] direction

For air flow in the [111] direction of the BCC lattice of cells, the representative cell is a prism with equilateral triangular sides, with the foam edges forming a 3_1 helix around the prism axis (Fig. 3b); the structure consists of 3 stacked sections, each twisted by 120° relative to the previous section. The length of the prism contains one complete turn of the edge helix, and the periodic end surfaces have the same orientation. The lateral faces of the prism are mirror symmetry planes. A second-order upwind discretization scheme was used in the CFD, with the over-relaxation factors for density and momentum reduced from the default values to achieve convergence.

5. Results of CFD

5.1. Flow through the wet Kelvin model in the 001 direction

A vector map shows the velocities at every other grid point (Fig. 4a) in a prism of length $\sqrt{2}L$. the maximum velocity in this simulation is 2.63 m s^{-1}. The flow changes direction to pass almost perpendicularly through the hole in the diagonal hexagonal face. This occurs in spite of there being a 'line of sight' through these holes, parallel to the z axis. There is a near-zero velocity region downstream of the half Plateau-border edge, perpendicular to the z axis, seen in the lower right of the figure, and a similar flow stagnation zone upstream of the related edge at the prism exit. CFD of the prism of length $2\sqrt{2}\,L$ (Fig. 3a) produces a velocity pattern that repeats in each half, being reflected about a plane that contains the z axis and bisects the prism. Consequently it is only necessary to analyse the flow in the shorter prism, making the CFD solution more rapid.

The total pressure contour map (Fig. 5a) is the periodic part of the solution, after the constant pressure gradient has been removed. There are large regions where the pressure (in Pa) is $1 > p > -1$, indicating a nearly uniform pressure gradient through the foam.

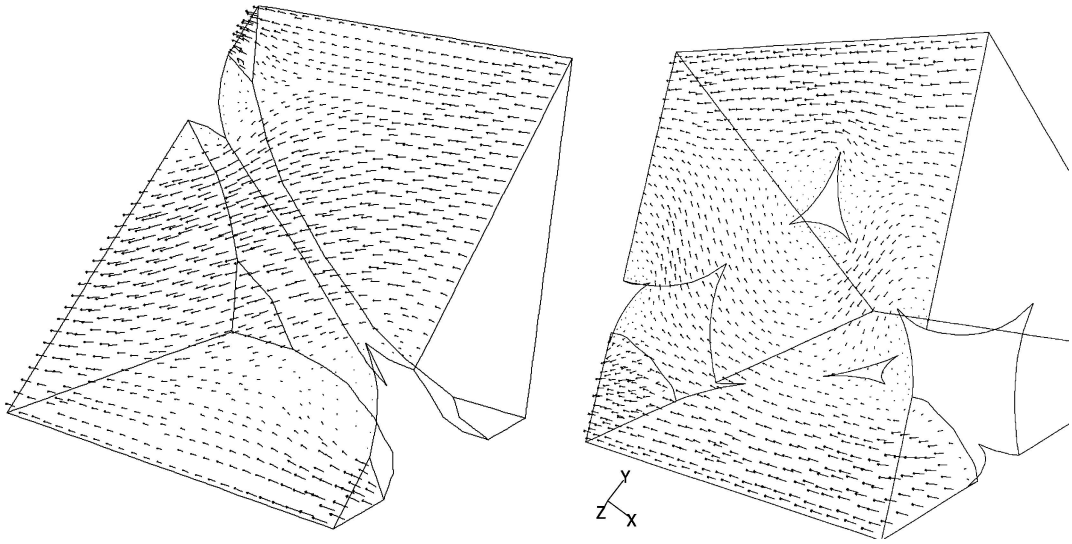

Figure 4 Velocity vectors for laminar flow in a wet Kelvin foam with $S = 0.3$, $D = 0.6$ mm, under pressure gradient 10 kPa m^{-1} in (a) [001], (b)[111] directions. For clarity, vectors are only shown on nearest symmetry face, and on the small periodic faces.

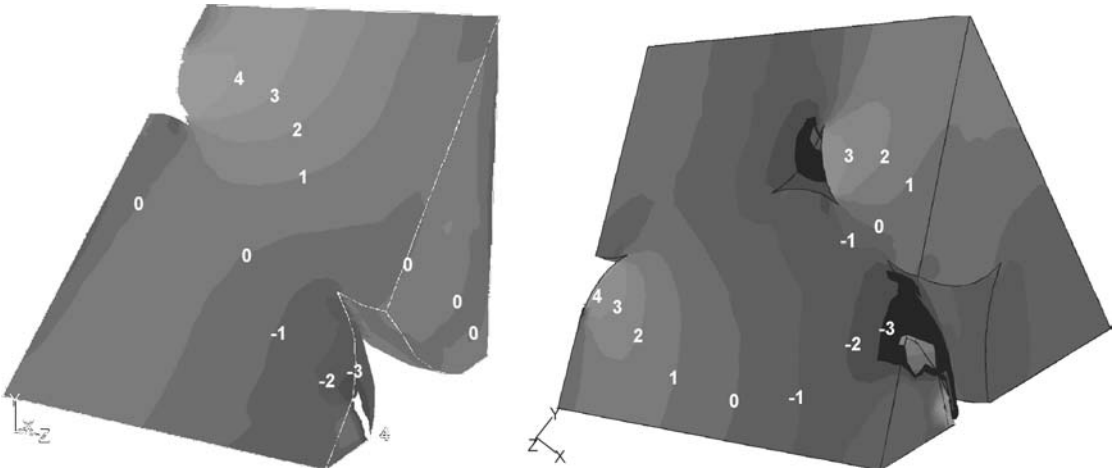

Figure 5 Contours (Pa) of the periodic part of the total pressure for flow in a wet Kelvin foam with $S = 0.3$, $D = 0.6$ mm, under pressure gradient 10 kPa m^{-1} in (a) [001], (b) [111] directions. The contours are shown on the visible faces of the prisms, which contain holes where the polymer structure fits.

The pressure drop across the 0.3 mm long prism shown. from the applied pressure gradient, is 3 Pa. The pressure rises to 5 Pa upstream of the Plateau border edge on the exit face of the prism, and sinks to −5 Pa downstream of the corresponding edge on the entry face of the prism.

Fig. 6 shows the predicted values of K as a function of the hexagonal face hole area, for cells of diameter 0.6 mm. The predicted K values are lower than the experimental data for the same hole area. The lowest point is for the Pudgee foam.

Predictions for cells of different diameters, for edge spread $S = 0.3$, are given in Table IV, and plotted against D_C in Fig. 7. This shows that K depends almost linearly on D_C, with a slightly S-shaped relationship. The S shape is less marked than that for the dry Kelvin model [10]. The velocity pattern changes with the cell diameter; the maximum velocity occurs at the centre of the hole in the diagonal hexagonal faces (Fig. 3a) for $D_C \leq 0.3$ mm, but at the exit/entrance hexagonal face holes for $D_C \geq 0.6$ mm.

5.2. Flow through the wet Kelvin model in the [111] direction

A computation was made for the edge spread parameter $S = 0.3$. The vector map shows the velocities at all the grid points on the diagonal side of the prism (Fig. 4b). The velocity field repeats in each third of the prism, with the pattern rotated by 120° about the length axis, as required. The flow changes direction to pass almost perpendicularly through the holes in

TABLE IV Predictions for Kelvin foam with $S = 0.3$, under a pressure gradient of 10 kPa m^{-1} as a function of cell diameter

Cell diameter D_C mm	Permeability K 10^{-9} m^2	Max velocity V_{max} m s^{-1}
0.15	0.16	0.21
0.3	0.61	0.82
0.6	1.83	2.59
0.9	2.82	4.78
1.2	3.67	7.02
2.0	5.31	11.78

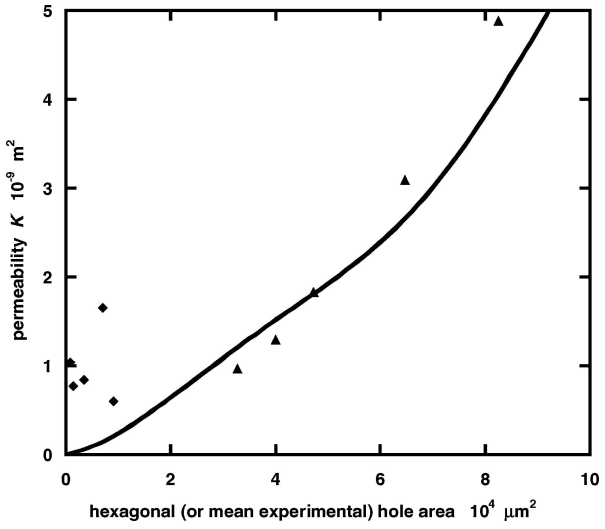

Figure 6 Permeability K vs. mean cell face hole area: (◆) PU foams of cell diameter $D_C \approx 0.5$ mm, (▲) CFD for wet Kelvin foam, curve CFD for dry Kelvin foam, with $D_C = 0.6$ mm.

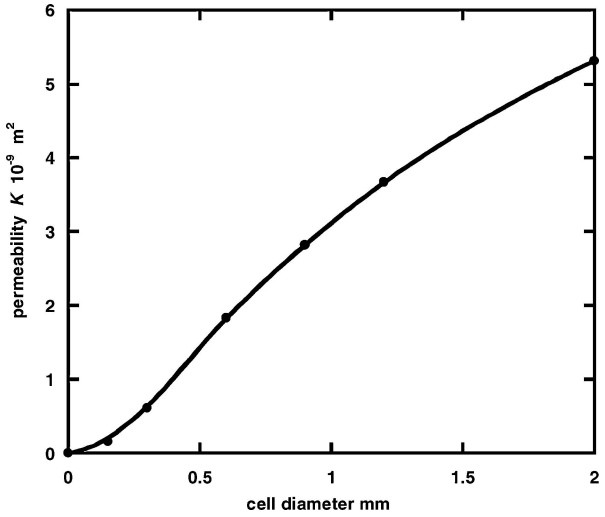

Figure 7 Permeability K vs cell diameter, for wet Kelvin foams with $S = 0.3$.

the hexagonal faces. The total pressure contour map (Fig. 5b) shows a maximum pressure of 4 Pa upstream of a Plateau border edge, perpendicular to the main flow direction, and a minimum of −4 Pa downstream of similar edges. The permeability was $K = 1.836 \times 10^{-9}$ m^2, the same within 1% as for the [001] direction flow, hence the foam model appears to have an isotropic permeability.

6. Airflow measurements

For the upholstery or compressed chip PU foam, values of B are positive. However for the slow recovery foams, the inertia coefficient B is negative (Table V). This was deduced [10] to be due to cell face deformation at high pressure gradients.

TABLE V Air-flow parameters for slow recovery PU foams

Foam	Permeability K 10^{-9} m^2	Air inertia B μm
Royal medica	1.65 ± 0.50	−100 ± 78
Sunmate soft	0.84 ± 0.26	−560 ± 480
Sunmate medium	0.77 ± 0.15	−260 ± 370
Sunmate firm	1.04 ± 0.42	−650 ± 620
Pudgee	0.60 ± 0.19	−73 ± 8

7. Discussion

Equation 2 predicts a permeability of 31×10^{-9} m^2 for a 1 mm cell size, independent of the hole size. The Gent-Rusch model geometry differs from that of PU foams; the latter have a variety of flow paths through face holes, and faces at angles to the applied pressure gradient. In contrast, the wet Kelvin model geometry is close to that of the real foam; it has changes in air-flow direction, with the splitting and merging of air flows. However, it lacks any variation in cell shape and size, and all faces are assumed to contain holes. Fig. 6 shows that K increases with hole area. The PU foams have a wide range of hole areas; their permeability probably depends on the area of the largest hole in each cell, and on linked paths between large holes. Consequently K will depend on a statistical average of hole area towards the upper end of the distribution, rather than on the mean hole area. The model also assumes that there is a hole in every face, which is not true for the PU foams. This factor, if incorporated in the model, would reduce the predicted K values, so cannot explain the discrepancy between the predictions and the experimental data.

The wet Kelvin foam model predicts values of K that are the same within 10% as for the dry Kelvin foam model [10], for the same hexagonal face hole area. The dry Kelvin model has a zero polymer volume fraction, and the flow patterns differ from those of the wet Kelvin model; the latter has stagnant flow areas upstream and downstream of edges that are perpendicular to the general flow direction, but the former has no such stagnant areas. Hence the main factors that determine the permeability must be the cell size and the cell hole area, and not details of the edge cross-section shape.

Boosma *et al.* [9] also used an idealised, but slightly less regular (Weaire-Phelan), model for the foam structure. They generated the foam geometry using Surface Evolver, but used a different CFD package to perform the analysis. The aluminium foam that they modelled had a lower relative density (0.04) and a larger mean cell diameter (2.3 mm) than the PU foams modelled here. Consequently it is not easy to compare the permeability of 3.6×10^{-9} m^2 (calculated from their predicted pressure gradient for water flow) with the results of the CFD described here, except to say that it is of the same order of magnitude as the prediction in Fig. 7 for $D_C = 2$ mm. Since they considered a single cell size and a single foam relative density, they were unable to comment on the effects of cell size and cell hole size.

The wet Kelvin foam geometries generated have also been used for Finite Element Analysis of the large strain compression of the solid foam; this will be reported in a separate paper.

8. Conclusions

CFD predicts foam permeabilities K, for laminar air-flow through a wet Kelvin foam model with regular cell hole sizes, that are lower than experimental data for foams with the same mean hole diameter and cell size. The predicted K value depends almost linearly on the cell diameter, while, at a fixed cell size, there is an almost linear increase in K with the cell hole area. The permeability of the PU foams is probably a function of the area of the largest holes in the cells. The predicted air flow permeability for the wet Kelvin model is the same in the [001] and [111] directions to within 1%, so the model appears to be isotropic.

Acknowledgments

The author is grateful to K. Braake for a copy of wet-foam.cmd for use with Surface Evolver.

References

1. N. J. MILLS and G. LYN, *Cell. Polym.* **21** (2002) 343.
2. R. E. JONES and G. FESMAN, *J. Cell. Plast.* **1** (1965) 200.
3. A. N. GENT and K. C. RUSCH, *J. Cell Plast.* **2** (1966) 46.
4. N. C. HILYARD and P. COLLIER, *Cell. Polym.* **6** (1987) 9.
5. W. THOMSON, *Phil. Mag*, **24** (1887) 503, reproduced in *The Kelvin Problem*, edited by D, Weaire (Taylor and Francis, London, 1996).
6. K. A. BRAKKE and J. M. SULLIVAN, Using symmetry features of the Surface Evolver to study foams, in "Mathematics and Visualisation", edited by K. Polthier and H. C. Hege (Springer Verlag, Berlin, 1997).
7. A. M. KRAYNIK, M. K. NEILSEN, D. A. REINELT and W. E. WARREN, in "Foams and Emulsions", edited by J. SADOC and N. RIVIER, (Kluwer, 1999) p. 259.
8. J. G. FOURIE and J. P. DU PLESSIS, *Chem. Eng. Sci.* **57** (2002) 2781.
9. K. BOOMSMA, D. POULIKAKOS and Y. VENTIKOS, *Int. J. Heat & Fluid Flow.* **24** (2003) 825.
10. C. FITZGERALD, I. LYN and N. J. MILLS, *J. Cell. Plast.* **40** (2004) 89.
11. J. A. F. PLATEAU, "Statique experimentale et theorique des liquides soumis aux seules forces moleculaires" (Gauthier-Vilars, Paris 1873).
12. R. PHELAN, D. WEAIRE and K. BRAKKE, *Expt. Mat.* **4** (1995) 181.
13. H. X ZHU, J. F. KNOTT and N. J. MILLS, *J. Mech. Phys. Solids* **45** (1997) 319.

Received December 2004
and accepted April 2005